

# Holocene vegetation record of upland northern Calabria, Italy: Environmental change and human impact

The Holocene  
2019, Vol. 29(4) 633–647  
© The Author(s) 2019



Article reuse guidelines:  
sagepub.com/journals-permissions  
DOI: 10.1177/0959683618824695  
journals.sagepub.com/home/hol



Jan Sevink,<sup>1</sup> Corrie C Bakels,<sup>2</sup> Peter AJ Attema,<sup>3</sup> Mauro A Di Vito<sup>4</sup>  
and Ilenia Arienzo<sup>4</sup>

## Abstract

Earlier studies on Holocene fills of upland lakes (Lago Forano and Fontana Manca) in northern Calabria, Italy, showed that these hold important palaeoecological archives, which however remained poorly dated. Their time frame is improved by new <sup>14</sup>C dates on plant remains from new cores. Existing pollen data are reinterpreted, using this new time frame. Two early forest decline phases are distinguished. The earliest is linked to the 4.2 kyr BP climatic event, when climate became distinctly drier, other than at Lago Trifoglietti on the wetter Tyrrhenian side, where this event is less prominent. The second is attributed to human impacts and is linked to middle-Bronze Age mobile pastoralism. At Fontana Manca (c. 1000 m a.s.l.), it started around 1700 BC, in the higher uplands a few centuries later (Lago Forano, c. 1500 m a.s.l.). In the Fontana Manca fill, a thin tephra layer occurs, which appears to result from the AP2 event (Vesuvius, c. 1700 BC). A third, major degradation phase dates from the Roman period. Land use and its impacts, as inferred from the regional archaeological record for the Raganello catchment, are confronted with the impacts deduced from the palaeoarchives.

## Keywords

4.2 ka BP climate event, archaeology, lake fills, pollen records, tephrochronology

Received 20 May 2018; revised manuscript accepted 3 December 2018

## Introduction

Within the scope of the Raganello Archaeological Project (RAP) of the Groningen Institute of Archaeology (GIA), Holocene fills from several high-altitude depressions and lakes in northern Calabria (Figure 1a and b) were studied for their pollen and other microfossils, with emphasis on the impacts of early land use. Among these, Lago Forano (LF) and Fontana Manca (FM) in the Monte Sparviere area (Figure 1b) were found to be the only ones holding pre-Roman sediments (Feiken, 2014). The results were presented in several publications (Attema et al., 2010; Feiken, 2014; Kleine, 2004; Kleine et al., 2005; Woldring et al., 2006), but remained tentative. The main reason was that most <sup>14</sup>C datings had not been performed on macro remains of terrestrial plants (AMS), but on bulk samples. The reliability of such datings is open to discussion (see e.g. Sevink et al., 2013), particularly while some age reversals were observed. Nevertheless, it was clear that LF held a potentially complete Holocene record, while the record from FM was apparently shorter but still covered an interesting part of the middle-Holocene.

Establishing the Holocene vegetation record for the upland landscape of northern Calabria has specific relevance for the evaluation of potential early human impacts at regional scale. Proxies for such impacts are the increase in the number of settlements and sites recorded in archaeological studies (Attema et al., 2010). While it is known from historical sources that a major Roman transhumance route passed through the area, it has been hypothesized that in preceding periods the uplands were used for mobile pastoralism, based on mounting evidence for the presence of late-Neolithic and early-Bronze Age ceramic find spots in the nearby upper valley of the Raganello River (De Neef, 2016; Ippolito, 2016a).

Holocene pollen records for the higher interior parts of mainland Southern Italy are rare. Lago Trifoglietti at 1048 m a.s.l. (Joannin et al., 2012) is nearest to the Raganello area (see Figure 1a), but it is from the humid Tyrrhenian slope of the Apennines (annual precipitation of 1850 mm), whereas annual precipitation in the Monte Sparviere area is considerably lower. Other cores are at far larger distances, such as the Lago Grande di Monticchio (see Figure 1a, at 650 m a.s.l.; Allen et al., 2002), Lago Alimini Piccolo (at sea level near Otranto, Puglia; Di Rita and Magri, 2009) and Canolo Nuovo (at 945 m a.s.l. Reggio Calabria; Schneider, 1985). Given this situation we decided to re-core the Sparviere locations and to improve the radiocarbon dating by selecting aboveground macro remains of terrestrial plants or charcoal fragments and applying <sup>14</sup>C AMS dating. New cores were taken in 2013–2015. At FM, a distinct tephra layer was found that earlier remained unnoticed, but potentially allowed for an independent check of the <sup>14</sup>C dates obtained. In this paper, results are presented from the reinterpretation of the original pollen counts

<sup>1</sup>Institute for Biodiversity and Ecosystem Dynamics (IBED), University of Amsterdam, The Netherlands

<sup>2</sup>Faculty of Archaeology, University of Leiden, The Netherlands

<sup>3</sup>Groningen Institute of Archaeology, University of Groningen, The Netherlands

<sup>4</sup>Istituto Nazionale di Geofisica e Vulcanologia (INGV), Italy

## Corresponding author:

Jan Sevink, Institute for Biodiversity and Ecosystem Dynamics (IBED), University of Amsterdam, Sciencepark 904, 1098 XH Amsterdam, The Netherlands.

Email: j.sevink@uva.nl

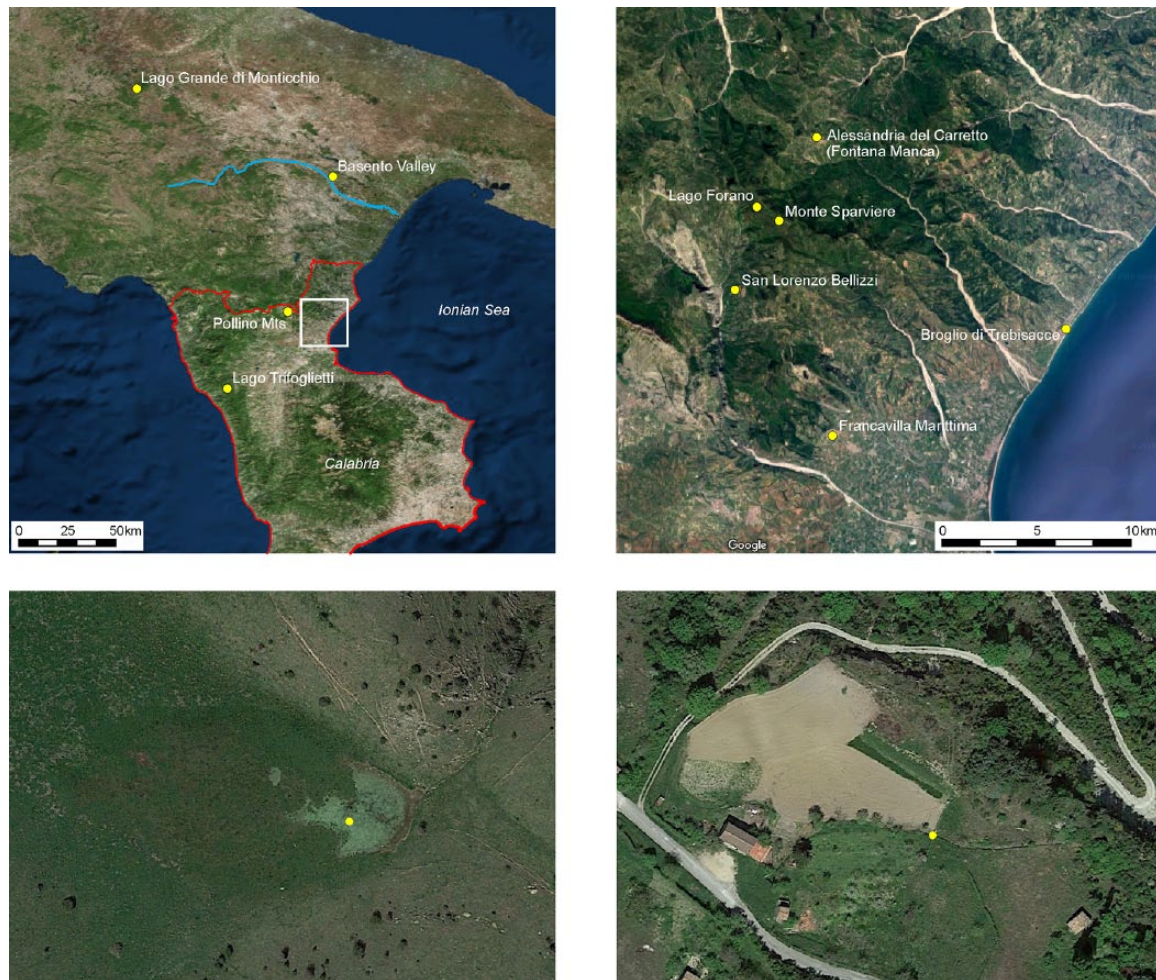


**Figure 1.** Locations of the area and sites. Left upper: Southern Italy and location of the area of study. Right upper: Area of study and location of Lago Forano and Fontana Manca. Left lower: Lago Forano and coring site (indicated by dot). Right lower: Fontana Manca coring site (dot).

within a more reliable time frame, based on existing and new  $^{14}\text{C}$  datings, on the identification of the tephra layer, and on the relation between the existing archaeological record and the vegetation history.

## Study area

### Topography

The LF and FM sites are located in the Monte Sparviere range (max. altitude 1713 m a.s.l.), in the eastern part of the Pollino Massif and facing the Ionian Sea. LF is a former small lake, which still holds some shallow open water during the wet season and is situated near the crest of the range at 1530 m a.s.l. (see Figure 1b and c). Drainage is to the NE through a narrow gap cut into a low ridge with exposed hard sandstone beds. LF covered a considerably larger area than the former lake at FM, which is a very small sediment-filled depression on the slope immediately below the northern outskirts of Alessandria del Carretto (see Figure 1b and d). This former, truly little lake, at 960 m a.s.l. lies in the most northern extension of the Sparviere range at about 5 km from LF.

### Climate

Because of its vicinity to Alessandria del Carretto, climatic data for FM are excellent: mean annual temperature is  $11^{\circ}\text{C}$  and annual precipitation is 826 mm (<https://it.climate-data.org>: 1982–2012). Its ombrothermic diagram is given in Figure 2. For comparison, this figure also shows the diagram for San Lorenzo Bellizzi, to the west of the Sparviere Range, which is rather identical to FM's

ombrothermic diagram. For LF, which lies in a remote area, no data are available. However, precipitation in the Sparviere Range is known to be distinctly lower than in the main Pollino Massif, being shielded by this massif against the relatively wet Tyrrhenian air masses that come in from the west during the rainy season (Brandmayr et al., 2002). Assuming a gradient of  $0.6^{\circ}\text{C}$  per 100 m, which is realistic for such drier range, mean annual temperature at LF will be of the order of  $7^{\circ}\text{C}$ . Annual precipitation is likely in the order of 1000 mm.

### Geology

The Monte Sparviere Range largely consists of flyschoid rocks from the Albidona Formation, which in this area is the dominant geological unit (Cesarano et al., 2002) and would be of Eocene age (Baruffini et al., 2000). In broad lines, three lithotypes are distinguished: (1) a lower sandy-clayey member, which is about 850 m thick and consists of an alternation of fine sands and pelites with a grey-olive colour, (2) an intermediate calcaric-clayey-sandy member of similar thickness, composed of marls with intercalations of clays and sands and (3) an upper conglomeratic-sandy member of about 600 m composed of an alternation of sands and granitic conglomerates. In all three members, coarse-grained strata have the characteristics of grauwacke and are fairly dense and hard rocks, the coarser beds standing out because of their higher resistance.

The upper conglomeratic member dominates the crest area, including the LF and its surroundings, and rocks in this area are virtually free of calcium carbonate. The outlet of the LF, a little stream draining the former lake, cuts through parallel bedded and

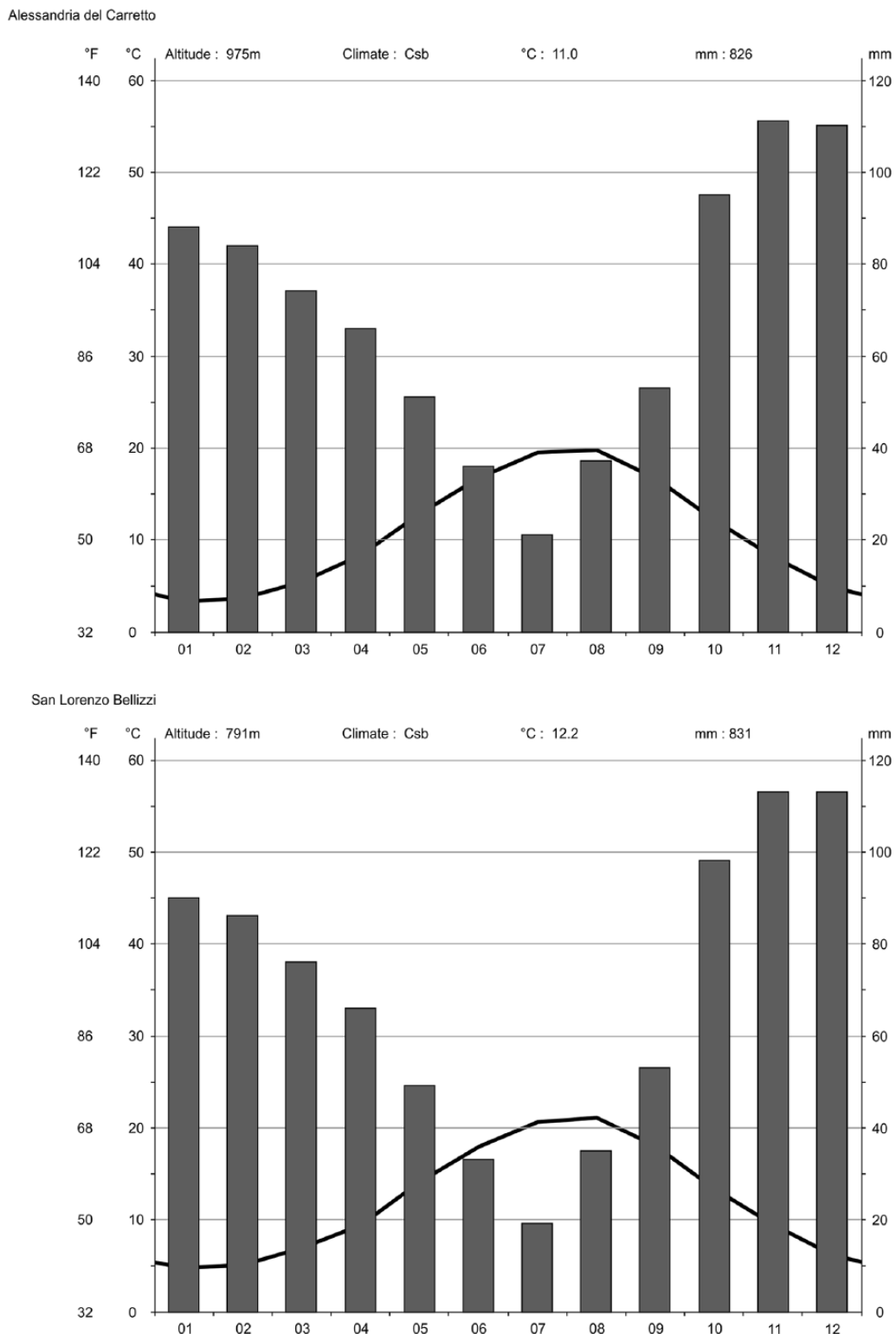


**Figure 2.** Ombrothermic diagrams for Alessandria del Carretto and San Lorenzo Bellizzi.

steeply inclined hard sandstone beds. A karstic origin of the shallow depression in which the lake formed can be completely excluded. Given its altitude (1530 m a.s.l.) and N–NE exposure it must be a nivation hollow or related glacial feature from the Pleistocene glacial periods (see e.g. Palmentola et al., 1990).

FM lies in the middle member, with marls as the dominant rock type, containing some calcium carbonate (finely divided, but also partly as fragments of calcite veins in the marls). Although a karstic origin cannot be fully excluded, local slumping or sliding causing a little valley to be blocked, seems to be the most likely explanation for the genesis of the lake.

In the Raganello Basin and adjacent part of southern Italy, thus far distal Holocene tephra have not been reported, but for an ash layer in the Basento Valley near Fosso La Capriola. This tephra was attributed to the Vesuvian AP3 eruption and would date from about 2800 cal. yr BP (Boenzi et al., 2008).

#### Vegetation

The actual Mediterranean vegetation is to a large extent affected by man. In Calabria, remnants of the original vegetation at higher altitude are preserved in the National Park of the Pollino. The

**Table 1.** Descriptions of the various corings from Lago Forano (above) and Fontana Manca (below).

Coring LF-1: Kleine			Coring LF-2: Sevink (2013)					
Depth (cm)	Material	<sup>14</sup> C Sample depth (cm)	Depth (cm)	Material	<sup>14</sup> C Sample depth (cm)			
0–210	Grey clay, from 160 cm soft	31–35 65–70 70–80 125–131.5 190–198	0–165	Dark humic clay				
210–240	Soft dark grey clay with wood fragments		165–195	Blueish grey clay with abrupt transition to				
240–265	Plastic clayey peat to peaty clay		195–266	Black/dark brown peat, slightly decomposed upper 5 cm	200–205			
265–315	Peaty clay with abundant wood fragments	271–275 275–278 310–315	266–271	Grey peaty clay	271–279			
315–405	Humic clay		271–279	Black/dark brown peat				
405–>465	Light grey clay to sandy clay (lower part)		279–325	Slightly decomposed clayey peat				
			325–>390	Slightly gravelly light grey humic clay	365–375			
Coring FM-1: Woldring et al.			Coring FM-2: Sevink (2013)			Coring FM-3: Sevink (2015)		
Depth (cm)	Material	<sup>14</sup> C sample depth (cm)	Depth (cm)	Material	<sup>14</sup> C sample depth (cm)	Depth (cm)	Material	<sup>14</sup> C sample depth (cm)
0–195	Anthropogenic layer		0–297	Greyish-blueish clay		0–300	Blueish-grey clay with some plant fragments and little stones and gravel	
195–225	Grey loam with organic remains		297–300	Peat	297–300	300–301.5	Transition towards clayey peat	
225–300	Dark humic to grey clay		300–301	Tephra		301.5–303	Very finely stratified peat	301.5–303
300–343	Peat	326–329	301–334	Peat		303–305	Tephra	
343–356	Grey humic clay		334–343	Finely laminated greyish peaty clay		305–325	Weathered but finely stratified blackish peat	314–316 328–330
356–375	Peat	372–374	343–389	Peat		325–345	Stratified peat with abundant wood	
375–450	Greyish-blueish clay with Ca-nodules		389–440	Greyish-blueish clay with Ca-nodules	388–393 seeds	345–352	Very finely laminated greyish peaty clay	
450–485	Greyish-blueish clay with Ca-nodules and gravel					352–>355	Stratified peat	

deciduous oaks downy oak, Turkey oak and Hungarian oak (*Quercus pubescens* Willd., *Q. cerris* L., *Q. frainetto* Ten.), the evergreen holm oak (*Quercus ilex* L.), oriental hornbeam (*Carpinus orientalis* Miller), sweet chestnut (*Castanea sativa* Miller), manna ash (*Fraxinus ornus* L) Montpellier maple (*Acer monspesulanum* L. and Italian alder (*Alnus cordata* Loisel.) characterize the vegetation between 800 and 1100 m. In the montane zone (1100–2000 m) deciduous oak species and sweet chestnut occur, while on the Ionian side several maple species (*Acer* sp.) can be found. Beech (*Fagus sylvatica* L.) grows in the upper part of this zone. Above 1500 m, silver fir (*Abies alba* Miller) occurs. Bosnian pine (*Pinus heldreichii* H. Christ syn. *leucodermis*) survives in the highest locations (Cocca et al., 2006; Gargaglione, 2001). Veenman (2002) studied the area where FM and LF are situated and analysed the actual vegetation along three transects running from 1100 m a.s.l. towards the coast. Between 1100 and 800 m, she noted a dominance of Turkey oak accompanied by beech, some sessile oak (*Quercus petraea* (Matt.) Liebl.), elm (*Ulmus minor* Miller) and, possibly planted, Aleppo pine (*Pinus halepensis* Miller). Hungarian oak and Italian alder were present as well. At lower ranges the vegetation was very much affected by human activity and grazing.

## Methods

### Field

At FM the original coring site (Woldring et al., 2006) was known with an accuracy of <1 m, whereas at LF the original site could not be established with that accuracy, landmarks being absent (Kleine et al., 2005). Here, accuracy will most likely have been <5 m from the original site. Sedimentary sequences were re-cored using a 6 cm gouge auger, with at LF a single core and a duplicate core at FM (taken at about 50 cm from each other). Cores were packed in fitting PVC tubes and transported to the Netherlands for separation of plant macro remains, charcoal and volcanic ash. Cores were described in the field. For descriptions, reference is made in Table 1.

### Sampling and dating

Cores from both sites were cut into slices of about 2–2.5 cm, depending on the sedimentary sequence and subsequently briefly boiled in a 5% KOH solution after which the series of samples was sieved over a 160 µm sieve to separate the 'coarser fraction'. Plant macro remains and charcoal were handpicked under the microscope from this coarser fraction. Suitable materials were

**Table 2.** Overview of the radiocarbon datings for Lago Forano and Fontana Manca. Sevink (2013) and Sevink (2015) refer to year of sampling, see Introduction and Table 1..

Sample nr	Depth (cm)	Material	Years (BP)	$\delta^{13}\text{C}$	Cal. yr AD/BC (95.4%)	Cal. yr BP (95.4%)	Source
Lago Forano early datings							
GrN 28466	31–35	Bulk	1180 ± 90		671–1013 AD	1280–937	Kleine (2004), Kleine et al. (2005)
GrN 27638	65–70	Bulk	3120 ± 210		1884–850 BC	3833–2799	
GrN 27639	70–80	Bulk	3190 ± 110		1742–1133 BC	3691–3082	
GrN 27075	121–131.5	Bulk	3140 ± 50		1508–1276 BC	3457–3225	
GrN 28043	190–198	Bulk	4660 ± 50		3630–3352 BC	5579–5301	
GrN 28044	271–275	Bulk	8740 ± 100		8203–7590 BC	10152–9539	
GrN 28045	275–278	Bulk	8790 ± 110		8213–7606 BC	10162–9555	
GrN 26794	310–315	Bulk	9220 ± 100		8709–8270 BC	10657–10219	
Lago Forano later datings							
GrA 34035	260–265	Base fraction	8485 ± 50		7592–7487 BC	9541–9436	Attema et al. (2010)
GrA 34036	260–265	Seeds	8590 ± 50		7722–7541 BC	9671–9490	
GrA 34039	271–275	Seeds	8770 ± 50		8170–7609 BC	10119–9558	
New Lago Forano							
GrA 64325	200–205	Seeds	4370 ± 60	–26.41	3326–2888 BC	5275–4837	Sevink (2013)
GrA 63112	271–279	Seeds	8525 ± 45	–27.84	7600–7519 BC	9549–9468	
GrA 63113	365–375	Seeds	9235 ± 50	–25.50	8598–8305 BC	10547–10524	
Fontana Manca early datings							
GrN 29415	326–329	Bulk	3710 ± 50		2278–1954 BC	4227–3903	Woldring et al. (2006)
GrN 30156	372–374	Bulk	3950 ± 65		2624–2209 BC	4573–4158	
New Fontana Manca							
GrA 64326	297–301	Seeds	1670 ± 90	–24.66	138–565 AD	1813–1386	Sevink (2013)
GrA 63450	388–393	Seeds	6975 ± 40	–24.71	5979–5751 BC	7926–7700	
GrA 66074	314–316	Willow wood	3540 ± 35	–27.66	1965–1754 BC	3914–3703	Sevink (2015)
GrA 66075	328–330	Willow wood	3705 ± 35	–27.73	2201–1980 BC	4150–3929	
GrA 66080	301.5–303	Charcoal	2955 ± 35	–25.00	1269–1047 BC	3218–2996	

washed and dried, and subsequently used for  $^{14}\text{C}$  AMS-dating. They are listed in Table 2.

Earlier  $^{14}\text{C}$  datings were largely traditional radiocarbon datings on whole samples of the organic matter fraction (see Table 2). Both these earlier data and the more recent AMS radiocarbon dating were carried out at the Centre for Isotope Research of Groningen University (CIO). Samples were pre-treated following the standard procedure (A-B-A, Brock et al., 2010). The dry weight of all AMS samples was more than 10 mg and therefore sufficient for  $^{14}\text{C}$  AMS-dating. The results were reported in conventional radiocarbon years, corrected for isotopic fractionation using the stable isotope ratio  $\delta^{13}\text{C}$ , and the conventional half-life (Mook and van der Plicht, 1999). For calibration into calendar age the recommended calibration curve IntCal013 (Reimer et al., 2013) was used, using the Oxcal4.3 software package (Bronk Ramsey, 2017). The  $^{14}\text{C}$  dates are reported in years BP and in cal. yr BC or cal. yr AD, with 95.4% significance. Only for the recent  $^{14}\text{C}$  datings CIO reported  $\delta^{13}\text{C}$  values. Where relevant, to allow for easy comparison with dates published in non-archaeological studies, we also report in cal. yr BP, with BP set at AD1950.

### Tephra

Tephra were separated by sieving, following on pre-treatment with 10%  $\text{H}_2\text{O}_2$ , after which coarse remaining organic fragments were removed by sieving (>2 mm) and sedimentation, followed by sieving over a 50  $\mu\text{m}$  sieve to remove fines. The fraction >50  $\mu\text{m}$  was dried and used for further analyses.

Strontium (Sr) isotope compositions were determined on handpicked feldspar and pyroxene crystals by Thermal Ionization Mass Spectrometry (TIMS) at the Istituto Nazionale di Geofisica e Vulcanologia, Osservatorio Vesuviano (Naples, Italy), using a ThermoFinnigan Triton TI multicollector mass spectrometer. Mineral samples of 0.2 g were washed several times in pure  $\text{H}_2\text{O}$  Milli Q<sup>®</sup>. After washing and dissolution by

high purity acid ( $\text{HF-HNO}_3\text{-HCl}$ ), Sr was separated by conventional ion-exchange chromatographic techniques. The Sr blank was of the order of 0.15 ng during the period of chemical processing. The measured  $^{87}\text{Sr}/^{86}\text{Sr}$  isotope ratios were normalized for within-run isotopic fractionation to  $^{86}\text{Sr}/^{88}\text{Sr} = 0.1194$ .  $2\sigma_{\text{mean}}$  that is, the standard error with  $N = 180$ , is better than  $\pm 0.000012$  for Sr measurements. During the collection of isotopic data, replicate analyses of NIST SRM 987 ( $\text{SrCO}_3$ ) were performed to check for external reproducibility. The external reproducibility ( $2\sigma$ , where  $\sigma$  is the standard deviation of the standard results, according to Goldstein et al., 2003) was  $0.710230 \pm 0.000019$  ( $2\sigma$ ,  $N = 120$ ). Sr isotope ratios of this work have been normalized to the recommended values of NIST SRM 987 ( $^{87}\text{Sr}/^{86}\text{Sr} = 0.71025$ ; Thirlwall, 1991).

### Palynology

The new cores were used to provide a better time frame for the two existing pollen studies (Kleine, 2004; Woldring et al., 2006). They have not been used for new pollen analysis. Samples have been treated with KOH, bromoform-ethanol gravity separation (s.g. 2.0) and acetolysis. Pollen was identified using Beug (2004), Moore et al. (1991) and a reference collection. Non-pollen palynomorphs were identified according to Van Geel (1978) and Van Geel and Aptroot (2006). For this study, the counts produced by Y. Boekema regarding FM and by E. Kleine regarding LF were entered in the programmes Tilia and TiliaGraph 2.0.41 (Grimm, 2015). New percentage diagrams were drawn based on an upland (dryland) pollen sum. *Salix*, *Poaceae* and *Cyperaceae* were left out because these taxa may have belonged, if only partly, to the wetland vegetation. *Alnus* was considered upland, because the only *Alnus* growing in the region is *Alnus cordata* Loisel, an upland tree. Pollen zones were drawn visually. Cereal pollen (*Poaceae* >40  $\mu\text{m}$ ) was discerned in LF and *Triticum/Hordeum* and *Avena* types in FM, but at least a part of this pollen may derive from wild grasses.

## Results and discussion

### Profiles and their dating

**FM.** The various corings at FM all exhibit exactly the same sedimentary sequence. About 3 m of grey clay to clay loam abruptly overlies peat, with a distinct stratigraphic hiatus evidenced by prominent decomposition and compaction of the peat immediately below the boundary (between c. 299 and 302 cm, see Figure 3). Differences in depth of this hiatus are minimal, as expected, considering the limited distance between the several corings. Differences in depth might even be (partly) because of the coring method used, leading to differences in compaction of the cored material (Dachnowsky corer by Woldring and others; gauge corer in 2013 and 2015).

Woldring et al. (2006) did not recognize the thin tephra layer that occurs a few centimetres below the hiatus in the top of the underlying peat (see Figure 3). The peat deposit has a somewhat variable thickness (75 cm: Woldring et al.; 92 cm in 2015), largely consists of finely stratified peat with abundant wood fragments, and holds an intermediate thin stratum (about 10 cm) of rather clayey peat to peaty clay. The peat abruptly overlies greyish blue clay with common gravel-size calcium carbonate nodules and some gravel to a depth of at least about 4.5 m.

$^{14}\text{C}$  dates are presented in Table 2. At first sight the dating of the thin peat layer immediately above the tephra layer seems problematic: the samples vary in age from cal. yr AD138–565 (core 2015, seeds, GrA 64326) to 1269–1047 cal. yr BC (core 2016, charcoal, GrA 66080). Given the fact that the upper part of the peat exhibits prominent decomposition, these results can be interpreted as follows: the charcoal represents the remains of peat that disappeared because of strong decomposition under aerobic conditions prior to the phase in which the overlying clay was deposited. The seeds postdate this phase of decomposition, being very well preserved, and most probably are the remains of vegetation present at the onset of the phase in which the clay was deposited. The difference in age between these two samples, therefore, can be seen as a reliable indication for the length of the sedimentary hiatus.

This thin tephra layer is shown in Figure 3, in which the overlying compacted and oxidized layer is also visible as black peaty material, lacking stratification. As for the age of this tephra layer, assuming a constant peat accumulation rate and taking into account some compaction and oxidation, it can be estimated at c. 1700 cal. yr BC (see Figure 4a). A slightly lesser age results for the top of the peat, which exhibits distinct compaction and oxidation (2–3 cm peat above the tephra layer), which would imply that a stratigraphic hiatus exists from between c. 1600 and 1700 cal. yr BC and the Imperial Roman period, after which the upper 3 m of clayey sediment was deposited.

As for the origin of the hiatus, it is very likely that peat growth came to a standstill because drainage improved either because of a drier climate or as a result of the natural development of such a small, temporary lake being filled up. Given the archaeological evidence, it is very well possible that the subsequent relatively massive accumulation of clay is because of artificial damming of the depression. In this area, devoid of natural springs, that would have ensured a continuous supply of water for its early inhabitants. However, testing these hypotheses would require further research into the archaeology and early history of Alessandria del Carretto.

For samples below the tephra layer, the plot of the various ages against depth (Figure 4a) clearly points to a fairly constant peat accumulation rate (c. 10 cm/century) and suggests that the earlier dating of GrN 29415 is reliable. In fact, the match between GrN 29415 and GrA 66075 is excellent ( $3710 \pm 50$  BP versus  $3705 \pm 35$  BP). Assuming that the age of sample GrN 29415 is indeed reliable, a significant hiatus exists around 380 cm, since

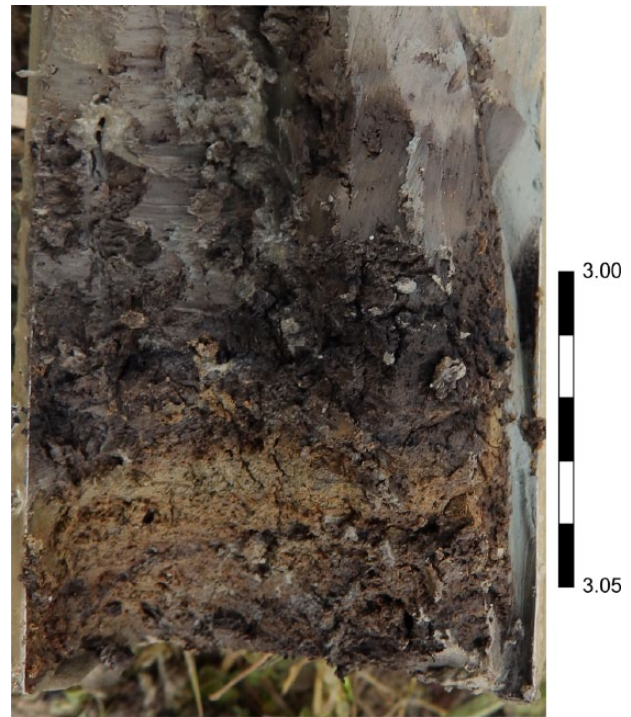


**Figure 3.** Detail of Fontana Manca core with tephra layer (core 2015). Depth is given in metres. For description, see core 2015, Table 1.

the seeds in the upper centimetres of the underlying clay date from around 5800 cal. yr BC. This suggests that the little lake originated shortly before 2500 cal. yr BC (4.5 cal. kyr BP).

**LF.** Descriptions of the two corings are presented in Table 1 and show that sedimentary boundaries and overall stratigraphy are similar: more or less peaty clay to peat, wedged in between clays. The upper boundary of the organic strata was at 210 (LF-1) and 195 cm (LF-2), respectively. In the recent coring (LF-2), this peat exhibited a slightly decomposed upper section, suggesting the presence of a stratigraphic hiatus. Whereas in coring LF-1 the lower boundary of the peat was at around 315 cm, it was found at 325 cm in coring LF-2. In both corings, sediments are non-calcareous, evidenced by the absence of a reaction with hydrochloric acid.

As described above, it was impossible to establish the exact original position of core LF-1, when taking the LF-2 core in 2012. The slight differences between the cores in depth and thickness of the peat thus can easily be explained because of the slight spatial variability in built up of the sedimentary sequence, in combination with differences in the coring methods used and associated differences in compaction.

In Figure 4b the results from the  $^{14}\text{C}$  datings are plotted against the sampling depth. For core LF-1 the problematic reliability of several  $^{14}\text{C}$  datings for the upper samples is evident. However,  $^{14}\text{C}$  ages obtained for the deeper samples from both cores – traditional  $^{14}\text{C}$  method on bulk samples for LF-1 and AMS method on seeds for LF-2 – and sedimentation rates, based on these datings, are nearly identical, strongly suggesting that for the peat sampled ages obtained are reliable for both cores. Based on extrapolation of the sedimentation rates, the peat sections would cover a time span from about 8500 cal. yr BC to about 3000 cal. yr BC, that is, about 5500 years.

Assuming a constant sedimentation rate for the specific types of sediment (peat and clay), the length of the hiatus between the upper clay layer and the peat can be estimated. This hiatus would be of the order of about 500 years at maximum, but whether this

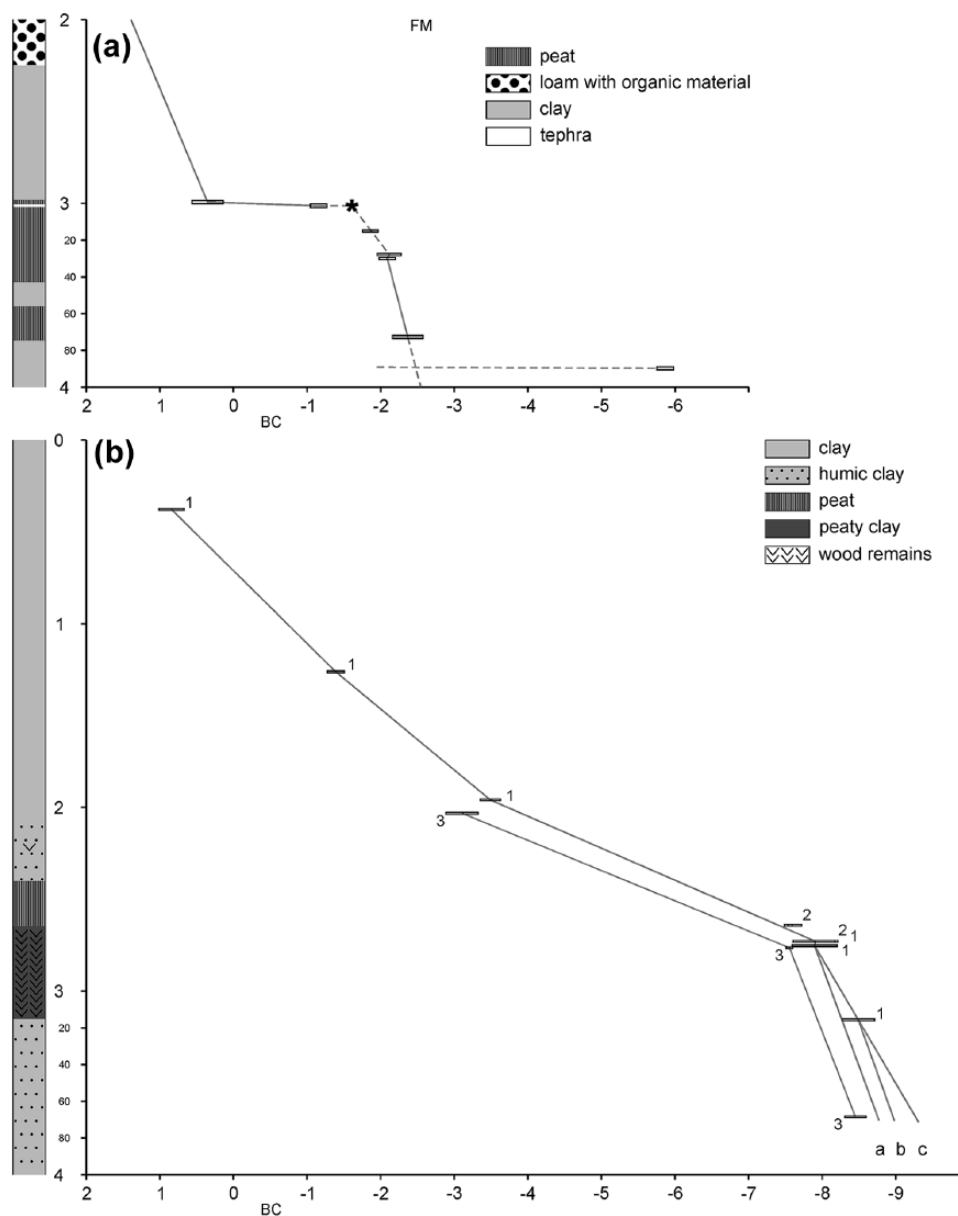


**Figure 4.** Depth in metres (Y-axis) versus age in kyr BC or AD (X-axis) for (a) Fontana Manca (FM) and (b) Lago Forano (LF).  $^{14}\text{C}$  ages are indicated by bars, showing the range at 95.4% probability. ★ = age of tephra based on extrapolated sedimentation rate. Numbers refer to cores as indicated in Table 1; a, b, and c refer to alternative extrapolations, based on sedimentation rates in cores 1 and 3.

is a true hiatus or the sedimentation rate gradually increased is not clear. As for its lower section, using the sedimentation rates found for cores LF-1 and -2, the sediment at 3.6 m depth can be tentatively dated. In Figure 4b, three alternatives are presented (a, b and c): a = rate of core LF-2 from 275 cm down, b = rate of core LF-2 but only for sediment below 315 cm and c = below 315 cm based on rate in core LF-1. Differences between these alternative ages are relatively small, and it is evident that the base dates from c. 9000 cal. yr BC (c. 11000 cal. yr BP), that is, the Preboreal.

**Comparison of sedimentation rates.** For the peat at LF an accumulation rate of c. 1 cm/80–85 years is calculated, which is considerably lower than at FM, where this rate is of the order of c. 1 cm/10 years. This probably reflects the major differences in origin and geology of the two lakes: LF is in a Pleistocene nivation hollow in relatively resistant grauwackes at truly higher altitude, whereas the lake at FM is in highly calcareous marls at distinctly lower altitude and was relatively short-lived, probably being formed by a mass movement that blocked a local valley or was accompanied by a rotational slip. Furthermore, it is clear that as a

whole the cores are marked by significant temporal variation in the sedimentation rate (Figure 4a and b) and, in the case of the FM core, holds a distinct stratigraphic hiatus.

**The tephra.** The measured  $^{87}\text{Sr}/^{86}\text{Sr}$  isotope compositions are 0.70793 for feldspar and 0.70767 for pyroxene crystals, values that in Figure 5 are plotted as vertical lines because we could not measure the Nd isotope compositions. The values are distinctly higher than those observed for the Ischia volcanic island and meet the values for the Somma-Vesuvius. As for the latter, distinction can be made between Somma-Vesuvius tephra from the past 39 ka BP and those from the AP eruptions (AP are eruptions that occurred between the Avellino and Pompei Plinian eruptions), characterized by higher Sr isotopic ratios. Products from the Campi Flegrei have not been considered, because they were quiescent during the interval of 2000–1000 cal. yr BC (4000–3000 cal. yr BP). Based on the  $^{14}\text{C}$  ages of the samples from the upper peat section of FM, this is the time interval within which the tephra was deposited, thus excluding a Phlegraean origin. More precisely, we estimated the age of the tephra at FM as roughly

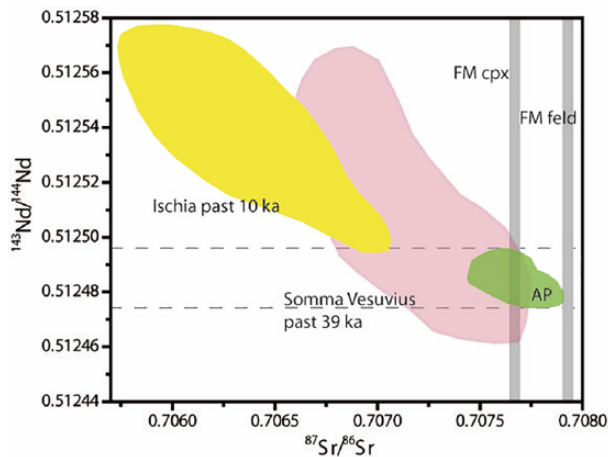


**Figure 5.** Sr-isotope versus Nd-isotope ratios. Fields are built on literature data for the Ischia volcanics (last 10 ka) and the Somma-Vesuvius volcanic rocks (last 39 ka). For the AP eruptions unpublished data are used (Arienzo). Sr isotope ratios of the minerals from Fontana Manca are represented as vertical lines. Data from the literature are from Cioni et al., 1995; Civetta et al., 1991; D'Antonio et al., 2013; Di Renzo et al., 2007; Iovine et al., 2017 cpx = clino pyroxenes; feld = feldspars (sanidine).

between 1600 and 1700 cal. yr BC and derived this age from the radiocarbon datings and calculated sedimentation rate (see above). In combination with this presumed age, the isotopic data clearly demonstrate the origin of the tephra: the AP2 eruption, which is the only AP eruption that occurred in the time gap mentioned (e.g. Passariello et al., 2010; Santacroce et al., 2008).

Quite some variation exists in the ages reported in various papers for this AP2 eruption. Vingiani et al. (2017) report an age of  $3170 \pm 240$  cal. yr BP, which was taken from Santacroce (1987). This is considerably younger than the age we obtained. However, Santacroce et al. (2008) reported 'a best available' age of the AP2 tephra of  $3500 \pm 40$  cal. yr BP ( $1550 \pm 60$  cal. yr BC). Furthermore, Passariello et al. (2010) report considerably earlier ages, published by Rolandi et al. (1998), and an age of 1730–1630 cal. yr BC (3680–3580 cal. yr BP) for a bone above the AP2 layer that they dated. Finally, Jung (2017), using dates for animal bones from below the AP2 layer but assumingly contemporaneous with this event, concluded that it dates from  $1689 \pm 24$  cal. yr BC, which is very similar to the age reported by Passariello et al. (2010). These more recently established ages are very much in line with our presumed age.

In this context, some attention needs to be paid to Boenzi et al. (2008), who described two tephra layers in their study of the relatively nearby Fosso La Capriola (Basento river basin, Basilicata). The oldest was identified as the Avellino tephra and the youngest as AP3 tephra. Although they report that the identification was based on the characteristic chemical and mineralogical composition, and glass particle morphology, data on these are not presented in their paper. The identification is seemingly based on a few  $^{14}\text{C}$  datings of charcoal fragments and an assumed  $^{14}\text{C}$  age of the Avellino eruption (3700 cal. yr BP), with the tephra layer encountered being younger than 3740 cal. yr BP and older than 3320 cal. yr BP. Recent studies show that the Avellino eruption is distinctly older (e.g. Sevink et al., 2011:  $3945 \pm 10$  cal. yr BP; Zanchetta et al., 2012: 3900–3800 cal. yr BP). We therefore do not exclude that Boenzi et al. (2008) erroneously identified the tephra layer as Avellino tephra, and that in reality this is a layer of AP2 tephra, similar to the tephra layer we found.

### Palaeoecology

**FM.** Figure 6 depicts the FM pollen diagram with the  $^{14}\text{C}$  data obtained as described above. Taxa not included are listed in the

Supplementary Table 1, available online (FM). The graphs represent three vegetation categories present in the wider region around the former lake: forest, secondary woodland and herbs. Dominant in the forest curve are deciduous oak species among which *Quercus cerris*-type is the most important. *Quercus robur*-type, which includes *Quercus pubescens* and *Quercus frainetto*, comes second. The next important taxon is *Ostrya*-type, which includes *Carpinus orientalis*. This picture is in agreement with the vegetation expected at the altitude of the lake: 960 m a.s.l. Another taxon mentioned for this altitude in the Pollino list presented above is *Alnus*. Pollen from *Acer* is present with one single grain and another characteristic tree, *Castanea sativa*, is only found in the upper part of the diagram. The tree taxa *Fagus*, *Abies* and *Pinus*, belonging to vegetation zones at higher altitude, are present as well, of which *Abies* is the most important.

Trees and shrubs like *Quercus ilex*, *Phillyrea*, *Pistacia* and *Olea* are considered as secondary growth, occurring when original forest is degraded. Within this category the *Quercus ilex* curve is the most important. These taxa may have replaced the original deciduous forest around FM, but the location is rather high for this supposition. This kind of pollen may have flown in with air currents from below when there was sufficient open space to allow this kind of transport. Veenman (2002) found *Quercus ilex* dominant at 750 m a.s.l.

**Zone 1.** From the lower clay only two horizons were counted. They indicate that deciduous forest prevailed around FM. The wetland taxa present a picture of a eutrophic lake with *Nymphaea*, surrounded by *Salix*. A date of cal. yr BC 5979–5751 was obtained for the upper part. A hiatus is supposed to separate zone 2 from zone 1.

**Zone 2.** The deciduous forest persists, but its composition has changed. The curve of *Quercus cerris* pollen is falling and the *Ostrya* percentages rise. *Fraxinus ornus* values have their optimum in this zone. *Fagus* and *Abies* curves rise as well. It looks as if the area around the lake is affected and becomes more open, giving opportunities to other species and catching more pollen from higher vegetation zones, for instance, *Abies*.

*Salix* disappears from the lake edge and the lake becomes shallower. Plants like *Potamogeton* and *Alisma* replace *Nymphaea* and peat formation sets in. The beginning of the change is dated 2624–2209 cal. yr BC.

**Zone 3.** During zone 3 the sediment becomes more clayey. The degradation of the forest continues. Secondary growth pollen percentages rise and the lake turns into a marsh with a sedge (Cyperaceae) vegetation including *Cladium*. Remarkable is the rise in *Sordaria* and *Sporormiella* spores, both indicators of the presence of dung.

**Zone 4.** This zone is remarkable for a maximum value in Poaceae pollen and a strong return of *Salix*. The deposition of clay has stopped and peat formation resumes. The rises in Poaceae and *Salix* may not represent anything dramatic, but may represent just another stage in the development of the vegetation in the lake and on its edge. Indications of open water are near absent. Dung indicators are very well represented. In addition to *Sordaria* and *Sporormiella*, *Chaetamium* and *Cercophora* were detected. The maximum of dung indicators is dated 2201–1980 cal. yr BC. The top of the zone, showing the transition to zone 5, is dated 1965–1754 cal. yr BC.

**Zone 5.** Zone 5 stands out for a strong decline in the values of upland tree species. Secondary vegetation and after that upland herb percentages show a rise. Herb pollen rises in percentages. It may very well be that the environment of FM is now seriously affected by man. However, such an interpretation should be

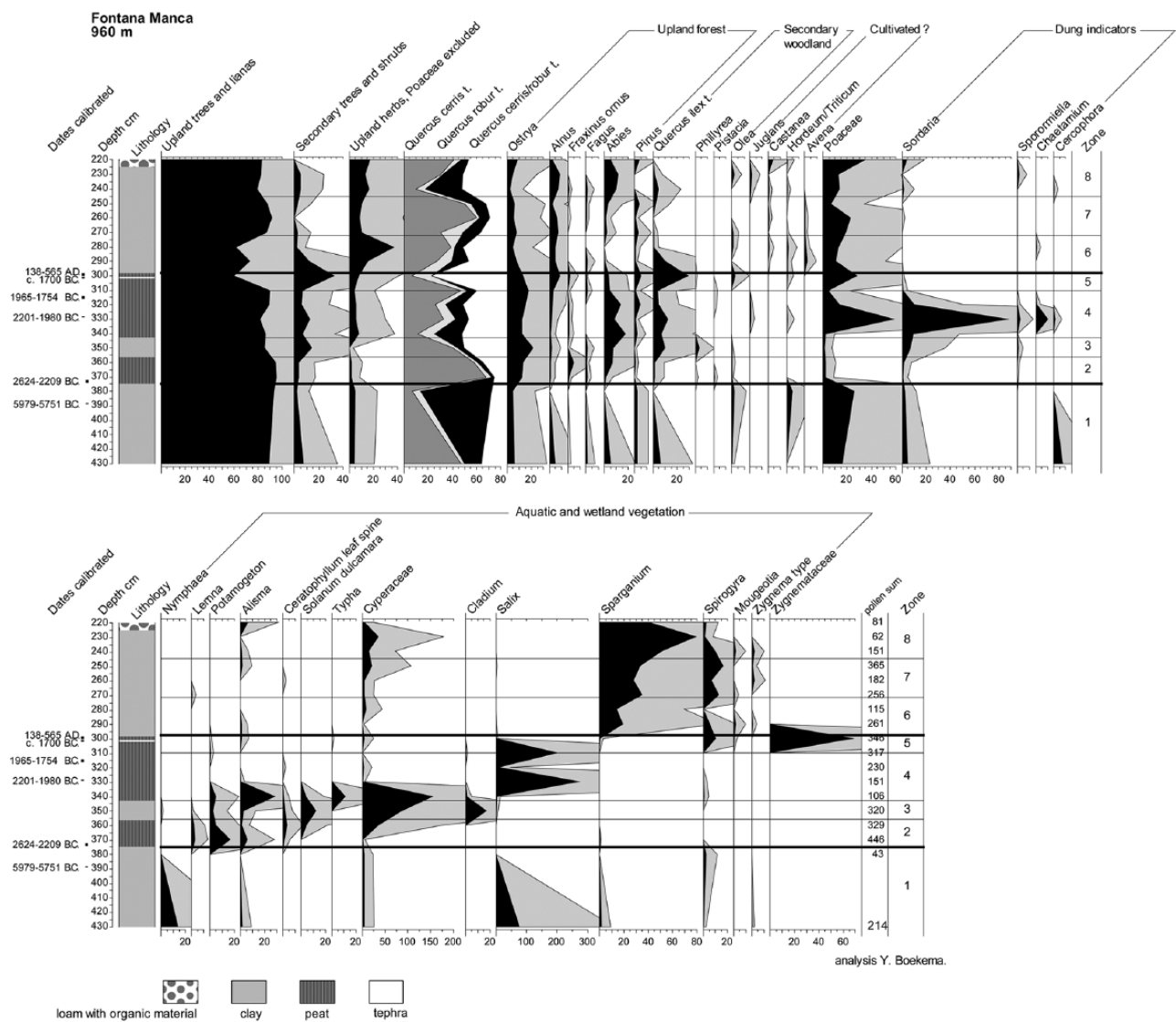


**Figure 6.** Pollen diagram for Fontana Manca.

looked at with caution. During the formation of the peat the AP2 ash was deposited. The resolution of the diagram, with only two spectra within this zone, is not sufficiently high to assess the influence of this event, dated at *c.* 1700 cal. yr BC, but it may have had some effect on the vegetation. The interpretation is not made easier because zone 5 ends with a serious hiatus. Peat formation in the depression is replaced by clay deposition. During zone 5 the depression was a marshy area with shallow pools as indicated by the presence of algae such as *Spirogyra*, *Mougeotia*, *Zygnema*-type and other Zygnemataceae.

**Zone 6.** Zone 6 is characterized by the lowest percentages of upland tree pollen and the highest percentages of upland herbs. This development is not because of deciduous *Quercus*, but because of the almost complete disappearance of *Abies*. A reason may be that pollen from this tree could not reach the depression because it got trapped in higher vegetation around the marsh, but this is unlikely. The belt of *Salix* has disappeared and upland herb pollen, which would have suffered from the same cause, rises in percentages. Zone 6 is also the zone where *Castanea* appears. Unfortunately, no date could be provided for the zone, but a hint is given by the  $^{14}\text{C}$  date of seeds embedded in the thin peat layer on top of the AP2 ash, namely cal. yr AD 138–565. If the seeds that provided the date got worked into the uppermost part of the peat during the first deposition of clay, this implies deposition from Roman times, or later, onwards. The seeds may have been trapped in the peat during the period of absence of deposition, but

this is less likely. They were in good condition and such seeds should be badly weathered if they had lain on the surface of a peat drying out. The depression became a marsh dominated by *Sparganium*.

**Zones 7 and 8.** Zone 7 shows a partial return of trees, especially of the oak *Quercus cerris* and *Abies*. The depression remains a wetland. The marsh persists during zone 8, but the oak pollen percentages again decline strongly and upland herb vegetation percentages rise. Dung indicators are present. *Abies* percentages rise, but this may be a relative rise because of a better chance of its pollen to get trapped in the sediment owing to the absence of higher vegetation around the marsh. Also, its pollen may have been washed in together with sediment that came down from eroding slopes higher up in the mountain, a possibility that must also be kept in mind regarding zones 6 and 7.

**LF.** LF is situated at a much higher altitude than FM, at 1530 m a.s.l. The pollen diagram is shown in Figure 7, and the taxa not presented there are listed in Supplementary Table 2, available online. The original author reports that she had difficulties with the attribution of *Quercus* pollen to its several types. Therefore, the values of *Quercus* pollen to its several types. Therefore, the values of *Quercus* pollen to its several types. Therefore, the values of *Quercus* pollen to its several types. Nevertheless, deciduous oak dominates the record and at first sight, this is surprising in regard to the altitude of the site. In general, more *Fagus* would have been

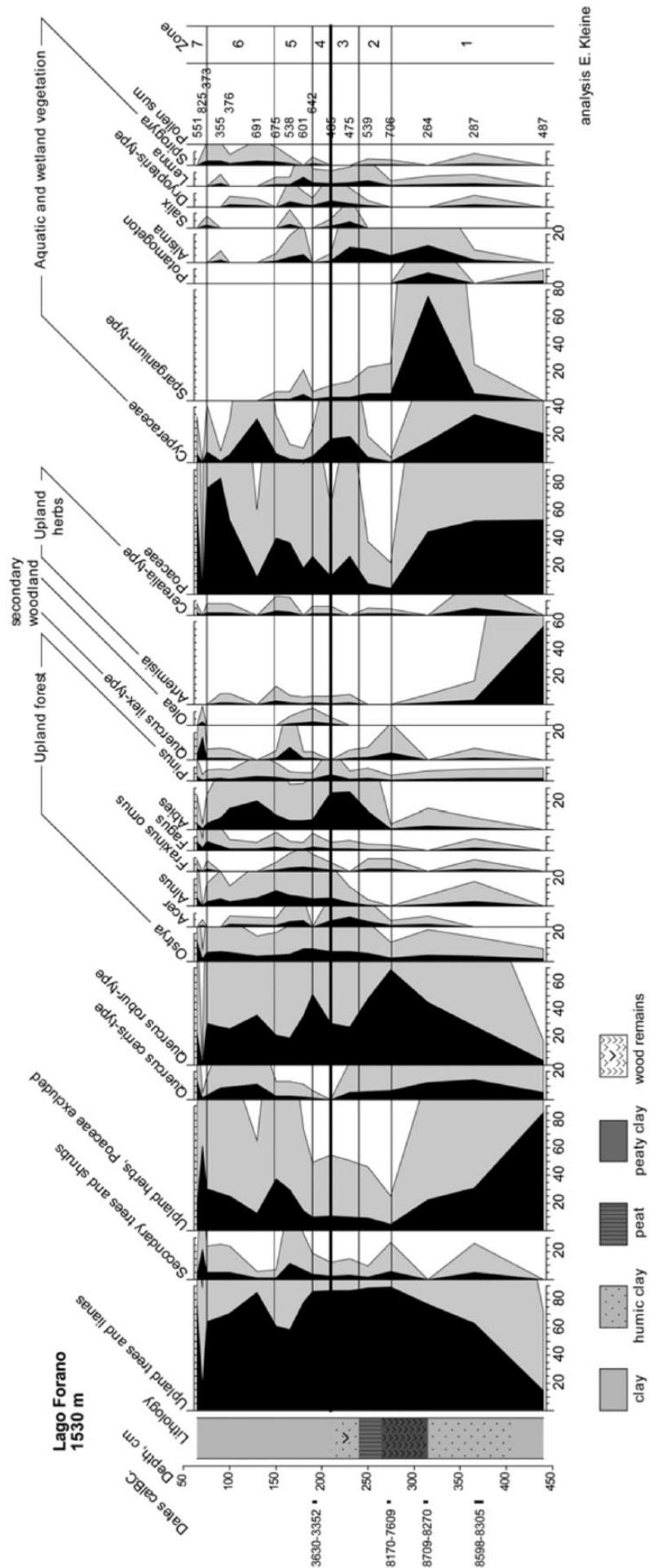


Figure 7. Pollen diagram for Lago Forano.

expected. However, the relative dryness of the region will have prevented the development of beech stands as the tree thrives best at around 1200 mm annual precipitation (Huntley et al., 1989).

**Zone 1.** The lowest zone is characterized by the transformation of the landscape from a steppe with *Artemisia* to a forest with deciduous trees, mainly *Quercus*. At the end of the zone, a belt of wetland plants such as *Sparganium* and *Alisma* surrounds the lake. Around 8709–8270 cal. yr BC the clayey sediment in the lake develops into peaty clay with wood remains.

**Zone 2.** In zone 2 the tree cover of the region reaches its maximum, but the relative share of *Quercus* falls, perhaps because of the appearance of *Abies*.

**Zone 3.** The zone is characterized by a relatively low *Quercus* and high *Abies* pollen percentages. The lake obtains a belt of *Salix* and, presumably, marsh ferns (*Dryopteris* type). Sedges (*Cyperaceae*) dominate the local vegetation in the lake. The sediment loses its peaty character. The boundary between zones 3 and 4 at 210 cm below surface is rather abrupt and as is suggested in 4.1.2, the presence of a hiatus of unknown length is likely.

**Zone 4.** From this zone upwards the deposition of clay dominates the record. *Quercus* pollen percentages rise again and those of *Abies* fall. A part of the marsh vegetation (*Salix* and *Alisma*) vanishes. The end is dated 3630–3352 cal. yr BC.

**Zone 5.** The values for *Abies* are low while the percentages of deciduous *Quercus* undergo a decline as well. The curve of herb pollen percentages rises. A temporary rise in *Fraxinus ornus*, *Quercus ilex* and *Olea* pollen percentages may indicate a phase of secondary forest during the events that led to open vegetation, but, as mentioned before, this pollen may not have been produced by the vegetation around the lake, but may have arrived from lower altitudes.

**Zone 6.** This zone reveals a return of forest, at least at its start, but this does not last. Herb percentages rise again and also a part of the Poaceae may originate from the dry terrain outside the lake. Algae, for instance *Spirogyra*, show that the lake still holds water.

**Zone 7.** The two uppermost spectra are very different from the rest. They originate from a depth of 65 and 70 cm below the present surface and may represent recent or sub-recent vegetation.

**Evaluation of the pollen records.** The lowest spectrum at LF indicates that deposition started in the late-Pleistocene with vegetation dominated by herbs, while the other spectra are to be ascribed to the Holocene. Forest composed of deciduous trees, and in a later stage silver fir (*Abies*), superseded the steppe. The conspicuous increase in relative abundance of *Abies* from 8000 to 7600 cal. yr BC onwards is not apparent in the Lago Trifoglietti diagram, obtained from a lake at 50 km distance as the crow flies, but is seen in the Lago Grande di Monticchio (Allen et al., 2002; Joannin et al., 2012). A series of fluctuations in the pollen record of the upland vegetation followed. After c. 3600–3300 cal. yr BC the surroundings of the lake lost a part of its tree cover (zone 5). Later, forest recovered, but a second phase of loss of trees followed. The question is whether these serious fluctuations are to be ascribed to climate, alteration of the soil characteristics or anthropogenic impact.

Since forest did return after the first tree decline in zone 5, severe degradation of the soil is very unlikely. An obvious cause would seemingly be anthropogenic impacts, but before reaching this conclusion, results from recent studies on the 4.2 cal. kyr BP

climatic event should be considered, which was a relative dry phase (Joannin et al., 2012). This event has been observed at many Italian sites south of 43°N, as described by Di Rita and Magri (2009) and by Zanchetta et al. (2016). It is also noted for Lago Trifoglietti (Joannin et al., 2012). The suggested cause is a natural phenomenon related to a general progression of a North African high-pressure cell affecting southern Italy. Very recently Di Rita et al. (2018) concluded that the event is the result of a complex interplay of different climate modes, additionally providing further evidence for its occurrence and age. This event may very well be the true cause for the first forest decline at LF, which starts at around 180 cm depth and is optimal around a depth that indeed corresponds with an age of c. 4.2 cal. kyr BP. The second decline of the forest, starting at c. 130 cm, can be dated at c. 1500 cal. yr BC, using the depth–age relationship for this part of the core (see Figure 4a).

The FM diagram does not represent the long stretch of time that is provided by LF. It covers its upper part, but with a higher resolution. An alteration and subsequent degradation of the original forest started in a period after 2624–2209 cal. yr BC. This phase is most likely contemporaneous with the first forest decline observed in LF and better dated. The presence of several dung indicators shows that concentrations of animals must have been present near the depression. The optimum of this forest decline was around 2201–1980 cal. yr BC. After 1965–1754 cal. yr BC the tree cover recuperated to some extent. Assuming that the forest decline is indeed because of a climatic event (a dry phase), it is possible that scarce remnants of pools attracted wild fauna. A concentration of wild animals may also have affected the local vegetation by intensive browsing and grazing, thereby reducing the tree growth still more. Alternatively, if the decline is attributable to anthropogenic exploitation of the environment, the dung indicators may point to the presence of herds of domestic animals. A third possibility is that the natural opening up of the forest made the area attractive to pastoralists and that the activity of their flocks added to the impact.

A second, still heavier, impact followed. During this phase the AP2 ash was deposited. According to the Trifoglietti data the climate was not extremely dry at that time. Peat growth continued after this event, and the impact may have been anthropogenic. However, the following hiatus hampers further interpretation. The occurrence of a hiatus is mainly apparent in the wetland part of the diagram. The arrival of a load of clay changed the local vegetation. As mentioned above, its start may be dated at cal. yr AD 138–565. In the upland pollen the only hint at a hiatus is provided by the appearance of *Castanea* (sweet chestnut) and this tree may support the dating.

Mercuri et al. (2013) discussed the history of *Castanea* as part of the OJC group (*Olea*, *Juglans*, *Castanea*). A definite rise in *Olea* (olive), *Juglans* (walnut) and *Castanea* pollen percentages indicates human activity; many pollen records show that *Juglans* and *Castanea* spread with the Roman culture (Mercuri et al. 2013). In the FM diagram *Olea* and *Juglans* are present before the clay deposition, but not with continuous curves. *Castanea* displays the rise which may indicate cultivation and this suggests a Roman date for the start of the sedimentation. However, it is not a definite proof. In the Trifoglietti diagram *Castanea* is present during the entire Holocene and rises only in the Middle Ages. Nevertheless, the combination of the <sup>14</sup>C date and the *Castanea* curve makes a Roman date for the arrival of clay likely.

#### Settlement intensity and human impact

The upland pollen cores of LF and FM are located at a short distance from the middle valley of the Raganello (Figure 1b). For this area, we have a substantial dataset of late pre- and protohistoric archaeological find spots that were inventoried in the course of the Raganello Archaeological Project and well dated on the



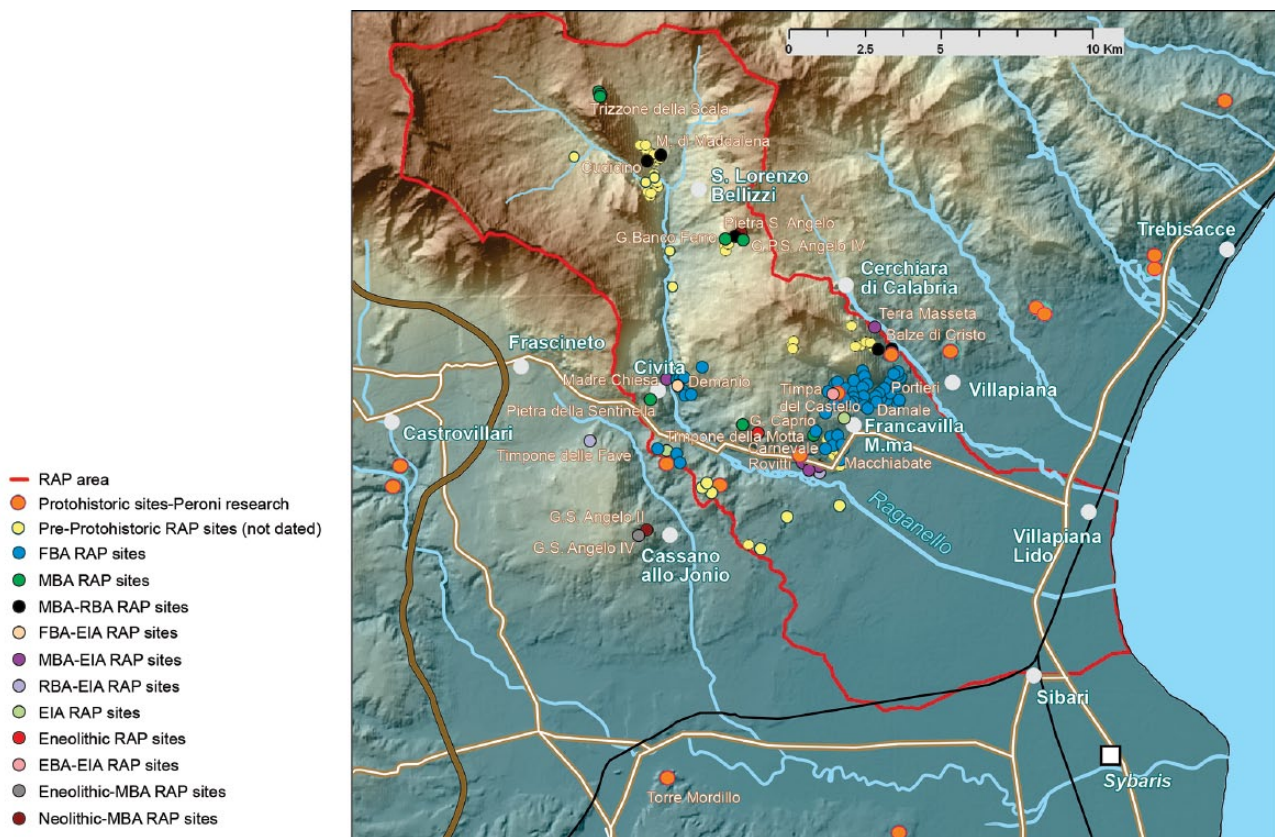


**Figure 8.** Settlement distribution in the Raganello catchment. For location of Fontana Manca and Lago Forano, see Figure 1b.

suggests that it is especially during the middle-Bronze Age 2 and 3 that settlement starts to spread over the valley and village communities start to fill in landscape niches suitable for a combination of subsistence farming and mobile pastoralism. Based on these archaeological data, this intensification of settlement and land use occurred in a relatively short period of ca. 200 years lasting to the final-Bronze Age–early-Iron Age transition around 1000 cal. yr BC, although a decline in settlement evidence already set in before the end of the Bronze Age (Ippolito, 2016a).

The increased settlement evidence for the middle-Bronze Age 2 and 3 periods rather postdates the second impact noted in the pollen record of FM, since that impact becomes already visible at c. 1700 cal. yr BC, suggesting an even earlier onset of human impact on the landscape because of settlement development at moderate altitudes. At LF the impact seems to be somewhat later, around 1500 cal. yr BC, more in line with the current archaeological evidence (see Table 4). Anyway, judging from this evidence, it is plausible that from that time on the middle-Bronze Age village communities in the middle Raganello valley exerted significant pressure on the vegetation in the nearby uplands.

Noteworthy in the archaeological record of the middle valley of the Raganello basin is the gradual decrease of settlement evidence during the last stages of the Bronze Age and the virtual absence of sites in the Iron Age (Ippolito, 2016a). This lack of settlement evidence in the uplands cannot be equated with lack of exploitation of the uplands: contemporaneous with the abandonment of the uplands we see a concentration of population in larger, so-called proto-urban settlements (Peroni and Trucco, 1994) in the final-Bronze age and early-Iron Age, located in the foothills overlooking the coast. Their rise is accompanied by rural infill surrounding these settlements (De Neef, 2016). Given the short distances from these sites to the uplands of LF and FM, it is likely that exploitation of the uplands continued, especially for more wide-ranging mobile pastoralism.

A recent study of the archaeozoological evidence from the proto-urban sites of Timpone della Motta at Francavilla Marittima and Broglio di Trebisacce indicates an important role for sheep/goat and cattle in the subsistence strategies of these two settlements from the middle-Bronze Age into the early-Iron Age (Elevelt, 2012). Geographically, increased exploitation by the community of Broglio di Trebisacce of the uplands around LF and FM for pastoralism is likely (Matteucci, 1984, for the importance of summer pastures and a hypothesis on drove roads between Broglio di Trebisacce and the uplands). Unfortunately, because of the hiatus in the pollen data, we are unable to link the growth of the proto-urban centres and their need for upland resources during the later-Bronze Age and Iron Age with environmental impacts in the uplands during this period.

The abandonment of the upland for settlement purposes lasted till the Hellenistic period when archaeological evidence for the existence of small farmsteads appears in the middle valley. In the vicinity of the FM core there is evidence for Roman settlement, most likely related to the historically known and long used transhumance route of the so-called ‘via della Reggia’ linking the coastal plain with the uplands. Diagnostic potsherds from Roman sites date to the period between the 1st century BC and the 1st century AD. Transhumance between the coastal plains of the Adriatic and the uplands is thus a likely cause for the impact on the vegetation that we see in the pollen data for the Roman period.

## Conclusion

The sedimentary sequences in the former lakes at LF and FM hold important archives that demonstrate several phases of forest decline. The first of these started after 2500 cal. yr BC and can be linked to the well-known 4.2 cal. kyr BP climatic event, which has been widely observed in the central Mediterranean basin. In the previous studies (Attema et al., 2010; Woldring et al., 2006),

this impact was ascribed to Bronze Age pastoralism, but the archaeological data indicate sparse settlement and this makes an important anthropogenic impact less likely.

A major early middle-Bronze Age anthropogenic impact is revealed by the second, heavier phase of forest decline present in both the FM and the LF diagrams, and its start dates from around 1700 cal. yr BC. This dating is well in line with the known archaeological record for the area and stresses the impact of this phase, first on the vegetation at medium altitude (FM), a few centuries later followed by the upland vegetation (LF).

Interestingly, during the early part of this second phase a thin layer of tephra from the AP2 eruption of the Vesuvius was deposited, which according to the most recent literature dates from  $1689 \pm 24$  cal. BC (Jung, 2017). This is the first recorded occurrence of this tephra in Calabria and represents a very useful tephrochronological marker, though some debate still exists on its age (see also Santacrose et al., 2008).

In the Roman period clay deposition smothered the FM depression, probably as the result of a severe human impact. A similar massive deposition of clay is also observed at LF, pointing to a general, massive disturbance of the upland vegetation and landscape, and concurrent soil degradation.

As described in the 'Introduction', Holocene pollen records from the southernmost parts of mainland Italy are rare. The important Lago Trifoglietti diagram was obtained from an area described by its authors as falling 'within the "lower mesotemperate bioclimate belt" of a temperate region and the ombrotype is upper hyperhumid' (Joannin et al., 2012: 1975). Both records reported here reflect the vegetation history of a drier region. One, FM, was obtained from an elevation comparable with Lago Trifoglietti, but the other one, LF, came from a much higher elevation. One of the results of the analysis of these depressions is that their palaeorecords exhibit the 4.2 cal. kyr BP event and, in the case of LF, does so even more prominent than Lago Trifoglietti. It is concluded that the drier climatic conditions characteristic for this event had a distinct impact on the already relatively dry uplands of Northern Calabria

### Acknowledgements

Sincere thanks are due to the authors of earlier pollen studies, E. Kleine, H. Woldring and Y. Boekema. Their pollen data were indispensable for our study and their help in the retrieval of these data is sincerely acknowledged, as is the aid by R. Cappers in this retrieval. M. van Leusen and A. Larocca, involved in the successive GIA projects in Calabria, helped us with finding the earlier coring locations. JS performed these new corings with the able help of M. den Haan, J. Wamsteker and N. Noorda. Radiocarbon data were produced by the CIO radiocarbon unit (Groningen) under the supervision of J. van der Plicht, who aided us with the evaluation of the datings that were earlier performed by this lab. B. van Geel and R. Cappers supported the identification and selection of datable plant macro remains from the new cores, while E.E. van Hees identified wood fragments, which were used for  $^{14}\text{C}$  dating. F. Ippolito provided the tables and figure holding the detailed information on the settlement chronology and distribution. E. Bolhuis, S. Tiebackx and J. Porck are thanked for producing the illustrations. Finally, we thank two anonymous reviewers for their comments, which helped to improve our manuscript.

### Funding

The author(s) received no financial support for the research, authorship and/or publication of this article.

### Supplemental material

Supplemental material for this article is available online.

### References

- Allen JRM, Watts WA, McGee E et al. (2002) Holocene environmental variability – The record from Lago Grande di Monticchio Italy. *Quaternary International* 88: 69–80.
- Attema PAJ, Burgers GJ and van Leusen PM (2010) *Regional Pathways to Complexity: Settlement and Land-use Dynamics from the Bronze Age to the Republican Period*. Amsterdam: Amsterdam University Press.
- Baruffini L, Lottaroli F, Torricelli S et al. (2000) Stratigraphic revision of the Eocene Albidona Formation in the type locality (Calabria Southern Italy). *Rivista Italiana di Paleontologia e Stratigrafia* [Research in Paleontology and Stratigraphy] 106: 73–98.
- Beug HJ (2004) *Leitfaden der Pollenbestimmung für Mitteleuropa und angrenzende Gebiete*. Munich: Pfeil.
- Boenzi F, Caldara M, Capolongo D et al. (2008) Late Pleistocene–Holocene landscape evolution in Fossa Bradanica Basilicata (southern Italy). *Geomorphology* 102(3): 297–306.
- Brandmayr P, Mingozzi T, Scalercio S et al. (2002) Stipa austroitalica garigues and mountain pastureland in the Pollino National Park (Calabria Southern Italy). In: Redecker B, Finck P, Härdtle W et al. (eds) *Pasture Landscapes and Nature Conservation*. Berlin; Heidelberg: Springer, pp. 53–66.
- Brock F, Higham T, Ditchfield P et al. (2010) Current pretreatment methods for AMS radiocarbon dating at the oxford radiocarbon accelerator unit (Orau). *Radiocarbon* 52(1): 103–112.
- Bronk Ramsey C (2017) OxCal 4.3. Available at: <https://c14.arch.ox.ac.uk/oxcal.html> (accessed 21 March 2018).
- Cesarano M, Pierantoni PP and Turco E (2002) Structural analysis of the Albidona formation in the Alessandria del Carretto-Plataci area (Calabro-Lucanian Apennines southern Italy). *Bollettino della Società geologica italiana* 1: 669–676.
- Cioni R, Civetta L, Marianelli P et al. (1995) Compositional layering and syn-eruptive mixing of a periodically refilled shallow magma chamber: The AD 79 Plinian eruption of Vesuvius. *Journal of Petrology* 36(3): 739–776.
- Civetta L, Galati R and Santacrose R (1991) Magma mixing and convective compositional layering within the Vesuvius magma chamber. *Bulletin of Volcanology* 53(4): 287–300.
- Cocca C, Campanile D and Campanile G (2006) Il parco nazionale del Pollino tra ecologia e sviluppo. *Forest@* 3(3): 310–314.
- D Antonio M, Tonarini S, Arienzo I et al. (2013) Mantle and crustal processes in the magmatism of the Campania region: Inferences from mineralogy geochemistry and Sr–Nd–O isotopes of young hybrid volcanics of the Ischia island (South Italy). *Contributions to Mineralogy and Petrology* 165(6): 1173–1194.
- De Neef W (2016) *Surface subsurface: A methodological study of metal age settlement and land use in Calabria (Italy)*. Unpublished Doctoral Dissertation, University of Groningen.
- Di Renzo V, Di Vito MA, Arienzo I et al. (2007) Magmatic history of Somma-Vesuvius on the basis of new geochemical and isotopic data from a deep bore-hole. *Journal of Petrology* 48(4): 753–784.
- Di Rita F and Magri D (2009) Holocene drought deforestation and evergreen vegetation development in the central Mediterranean: A 5500 year record from Lago Alimini Piccolo Apulia southeast Italy. *The Holocene* 19: 295–306.
- Di Rita F, Fletcher WJ, Aranbarri J et al. (2018) Holocene forest dynamics in central and western Mediterranean: Periodicity, spatio-temporal patterns and climate influence. *Scientific Reports* 8(1): 8929.
- Elevett SC (2012) *Subsistence and social stratification in Northern Ionic Calabria from the Middle Bronze Age until the*

- Early Iron Age: The archaeozoological evidence*. Unpublished Doctoral Dissertation, University of Groningen.
- Feiken H (2014) *Dealing with Biases: Three Geo-Archaeological Approaches to the Hidden Landscapes of Italy*. Groningen: Barkhuis Publishing.
- Gargaglione AA (2001) Geologia flora e vegetazione del massiccio montuoso del Pollino. *Basilicata Regione Notizie* 99: 17–24.
- Goldstein SL, Deines P, Oelkers EH et al. (2003) Standards for publication of isotope ratio and chemical data in chemical geology. *Chemical Geology* 202: 1–4.
- Grimm EC (2015) Tilia and Tiliagraph 2041. Available at: <https://www.tilias.com/download/> (accessed 21 March 2018).
- Huntley B, Bartlein PJ and Prentice IC (1989) Climatic control of the distribution and abundance of beech (*Fagus L*) in Europe and North America. *Journal of Biogeography* 16: 551–560.
- Iovine RS, Mazzeo FC, Arienzo I et al. (2017) Source and magmatic evolution inferred from geochemical and Sr-O-isotope data on hybrid lavas of Arso the last eruption at Ischia island (Italy; 1302 AD). *Journal of Volcanology and Geothermal Research*: 331: 1–15.
- Ippolito F (2016a) Before the Iron Age: The oldest settlements in the hinterland of the Sibaritide (Calabria, Italy) [Groningen]: Rijksuniversiteit Groningen. Available at: [https://www.rug.nl/research/portal/files/36137198/Complete\\_thesis.pdf](https://www.rug.nl/research/portal/files/36137198/Complete_thesis.pdf).
- Ippolito F (2016b) Contextualization of funerary evidence from the cave Sant'Angelo IV Northeastern Calabria Italy. *Palaeohistoria* 57–58: 111–116.
- Joannin S, Brugiapaglia E, Beaulieu JLD et al. (2012) Pollen-based reconstruction of Holocene vegetation and climate in southern Italy: The case of Lago Trifoglietti. *Climate of the Past* 8(6): 1973–1996.
- Jung R (2017) Chronological problems of the middle bronze age in Southern Italy. In: Lachenal T, Mordant C, Nicola T et al. (eds) *Le Bronze moyen et l'origine du Bronze final en Europe occidentale de la Méditerranée aux pays nordiques (xviii-xiii siècle avant notre ère)*. Strasbourg: Mémoires d'Archéologie du Grand-Est 1, pp. 621–639.
- Kleine E (2004) *Pollenonderzoek Lago Forano: Holocene vegetatiegeschiedenis van de Sibaritide*. Unpublished Master's Thesis, University of Groningen.
- Kleine E, Cappers R, Attema PAJ et al. (2005) Holocene vegetatiegeschiedenis van de Sibaritide (Calabrie Italie): Analyse van het pollenmateriaal uit Lago Forano. *Paleo-Aktueel* 14–15: 68–73.
- Matteucci R (1984) Pascoli estivi e tratturi nell'area di Broglio. In: Peroni R (ed.) *Nuove Ricerche Sulla Protostoria Della Sibaritide*. Roma: Publications du Centre Jean Bérard, pp. 260–265.
- Mercuri AM, Bandini Mazzanti M, Florenzano A et al. (2013) Olea Juglans and Castanea: The OJC group as pollen evidence of the development of human-induced environments in the Italia peninsula. *Quaternary International* 303: 24–42.
- Mook WG and van der Plicht J (1999) Reporting C-14 activities and concentrations. *Radiocarbon* 41(3): 227–239.
- Moore PD, Webb JA and Collinson ME (1991) *Pollen Analysis*. Malden, MA: Blackwell Science.
- Palmentola G, Acquafredda P and Fiore S (1990) A new correlation of the glacial moraines in the Southern Apennines Italy. *Geomorphology* 31: 1–8.
- Passariello I, Lubritto C, D'Onofrio A et al. (2010) The Somma-Vesuvius complex and the Phlaegrean Fields caldera: New chronological data of several eruptions of the Copper–Middle Bronze age period. *Nuclear Instruments and Methods in Physics Research Section B: Beam Interactions with Materials and Atoms* 268(7): 1008–1012.
- Peroni R and Trucco F (1994) *Enotri E Micenei Nella Sibaritide*. Taranto: Istituto Magna Grecia.
- Reimer PJ, Bard E, Bayliss A et al. (2013) IntCal13 and Marine13 Radiocarbon Age calibration curves 0–50,000 Years cal BP. *Radiocarbon* 55(4): 1869–1887.
- Rolandi G, Petrosino P and Mc Geehin J (1998) The interplinian activity at Somma–Vesuvius in the last 3500 years. *Journal of Volcanology and Geothermal Research* 82(1): 19–52.
- Santacroce R (1987) Somma-Vesuvius. *Quaderni Della Ricerca Scientifica* 114: 1–251.
- Santacroce R, Cioni R, Marianelli P et al. (2008) Age and whole rock–glass compositions of proximal pyroclastics from the major explosive eruptions of Somma-Vesuvius: A review as a tool for distal tephrostratigraphy. *Journal of Volcanology and Geothermal Research* 177(1): 1–18.
- Schneider R (1985) Analyse palynologique dans l'Aspromonte en Calabre (Italie meridionale). *Cahiers ligures de préhistoire et de protohistoire* 2: 279–288.
- Sevink J, Van Bergen MJ, Van Der Plicht J et al. (2011) Robust date for the Bronze Age Avellino eruption (Somma-Vesuvius): 3945 ± 10 calBP (1995 ± 10 calBC). *Quaternary Science Reviews* 30(9–10): 1035–1046.
- Sevink J, van der Plicht J, Feiken H et al. (2013) The Holocene of the Agro Pontino graben: Recent advances in its palaeogeography palaeoecology and tephrostratigraphy. *Quaternary International* 303: 153–162.
- Thirlwall MF (1991) Long-term reproducibility of multicollector Sr and Nd isotope ratio analysis. *Chemical Geology* 94: 85–104.
- Van Geel B (1978) A palaeoecological study of Holocene peat bog sections in Germany and the Netherlands based on the analysis of pollen spores and macro- and microscopic remains of fungi algae cormophytes and animals. *Review of Palaeobotany and Palynology* 251: 1–120.
- Van Geel B and Aptroot A (2006) Fossil ascomycetes in Quaternary deposits. *Nova Hedwigia* 82: 313–329.
- Veenman F (2002) *Reconstructing the Pasture a reconstruction of pastoral landuse in Italy in the first millennium BC*. Unpublished Doctoral Dissertation, Vrije Universiteit Amsterdam.
- Vingiani S, Minieri L, Albore Livadie C et al. (2017) Pedological investigation of an early Bronze Age site in southern Italy. *Geoarchaeology* 332: 193–217.
- Woldring H, Boekema Y, Attema PAJ et al. (2006) Vegetatieontwikkeling en landgebruik in de Monte Sparviere (Calabrie Italie). *Paleo-aktueel* 17: 82–89.
- Zanchetta G, Giraudi C, Sulpizio R et al. (2012) Constraining the onset of the Holocene 'Neoglacial' over the central Italy using tephra layers. *Quaternary Research* 78(2): 236–247.
- Zanchetta G, Regattieri E, Isola I et al. (2016) The so-called '42 event' in the central Mediterranean and its climatic teleconnections. *Alpine and Mediterranean Quaternary* 29(1): 5–17.